Water Research 258 (2024) 121770

Contents lists available at ScienceDirect

Water Research

journal homepage: www.elsevier.com/locate/watres

# Trade-offs between nitrogen and phosphorus removal with floodplain remediation in agricultural streams

Lukas Hallberg [a,*], Sara Hallin [b], Faruk Djodjic [c], Magdalena Bieroza [a]

[a] Department of Soil and Environment, Swedish University of Agricultural Sciences, Uppsala, Sweden
[b] Department of Forest Mycology and Plant Pathology, Swedish University of Agricultural Sciences, Uppsala, Sweden
[c] Department of Aquatic Sciences and Assessment, Swedish University of Agricultural Sciences, Uppsala, Sweden

ARTICLE INFO

*Keywords:*
Phosphorus
Denitrification
Stream remediation
Floodplains
Eutrophication

ABSTRACT

To improve water quality and reduce instream erosion, floodplain remediation along agricultural streams can provide multiple ecosystem services through biogeochemical and fluvial processes. During floodplain inundation, longer water residence time and periodic anoxic conditions can lead to increased nitrogen (N) removal through denitrification but also mobilization of phosphorus (P), impeding overall water quality improvements. To investigate the capacity for N and P processing in remediated streams, we measured potential denitrification and nitrous oxide production and yields together with potential P desorption and P fractions in floodplain and stream sediments in ten catchments in Sweden. Sediment P desorption was measured as equilibrium P concentration, using P isotherm incubations. Denitrification rates were measured with the acetylene inhibition method. Sediment nutrient process rates were combined with hydrochemical monitoring along remediated streams and their paired upstream control reaches of trapezoidal shape to determine the impact of floodplains on water quality. The correlation between floodplain denitrification rates and P desorption ($r = 0.53$, $p = 0.02$) revealed a trade-off between soluble reactive P (SRP) and nitrate removal, driven by stream water connectivity to floodplains. Nitrous oxide production was not affected by differences in P processing, but nitrous oxide yields decreased with higher denitrification and P desorption. The release of SRP from floodplains ($0.03 \pm 0.41$ mg P kg$^{-1}$ day$^{-1}$) was significantly lower than from trapezoidal stream banks ($0.38 \pm 0.37$ mg P kg$^{-1}$ day$^{-1}$), predicted by long-term SRP concentrations in stream water and floodplain inundation frequency. The overall impact of SRP release from floodplains on stream SRP concentrations in remediated reaches was limited. However, the remediated reaches showing increased stream SRP concentrations were also frequently inundated and had higher labile P content and coarse soil texture in floodplain sediments. To fully realize the potential for water quality improvements with constructed floodplains in agricultural streams, the promotion of denitrification through increased inundation should be balanced against the risk of P release from sediments, particularly in streams with high SRP inputs.

## 1. Introduction

Agricultural headwater streams are critical transport pathways for nitrogen (N) and phosphorus (P) losses in many catchments, causing freshwater eutrophication that poses a sustained threat to global water quality (Glibert et al., 2014; Le Moal et al., 2019) and stream ecology (Riseng et al., 2011). The combined effect of large bioavailable nutrient pools in soils and sediments, amassed from sustained intensive agricultural activities, and a changing climate projects a trajectory of accelerated N and P exports (Basu et al., 2022; Sharpley et al., 2013). Stream mitigation strategies, underpinned by an understanding of how they influence N and P cycling, are therefore critical to combat nutrient pollution and reach water quality targets (Bieroza et al., 2021; Keiser and Shapiro, 2019). As agricultural streams are typically trapezoidal-shaped channels with restricted riparian zones, there is a possibility to remediate them by excavating lateral floodplains to increase hydrological connectivity and biogeochemical processing capacity (Fig. S1; Powell et al., 2007). Floodplain remediation, also known as a two-stage ditch or compound channel, is a mitigation measure adopted in agricultural streams, which has a similar objective as floodplain reconnection in river restoration (Surridge et al., 2012). This measure relies on hydrological controls that increase water, solute and

* Corresponding author at: Department of Soil and Environment, Swedish University of Agricultural Sciences, Uppsala, Box 7014, 750 07, Sweden.
*E-mail address:* lukas.hallberg@slu.se (L. Hallberg).

https://doi.org/10.1016/j.watres.2024.121770
Received 24 October 2023; Received in revised form 17 April 2024; Accepted 11 May 2024
Available online 11 May 2024
0043-1354/© 2024 The Authors. Published by Elsevier Ltd. This is an open access article under the CC BY license (http://creativecommons.org/licenses/by/4.0/).

particulate residence times upon inundation during high flows (Bukaveckas, 2007). This increases biogeochemical reactivity, as vegetated floodplains offer active surfaces for sedimentation and nutrient processing (Hallberg et al., 2022; Mahl et al., 2015). Floodplain remediation has been shown to be more cost-efficient for removing N compared to constructed wetlands in Midwestern USA (Roley et al., 2016). Similarly, the implementation of this measure in Sweden has been shown to increase the potential for N removal (Hallberg et al., 2022).

In sediments, nitrate ($NO_3^-$) is permanently removed by reduction to nitrogenous gases via microbial denitrification, which may result in emissions of the greenhouse gas nitrous oxide ($N_2O$). However, saturated conditions in sediments that favor denitrification pose a risk for release of soluble reactive P (SRP) to the water column through desorption. The exchange of SRP between water column and sediments is largely controlled by redox-sensitive iron (Fe) oxides, adsorbing SRP from water column as ferric iron ($Fe^{3+}$) or releasing loosely bound SRP upon reduction to ferrous iron ($Fe^{2+}$; Simpson et al., 2020; Stutter et al., 2010). Under high SRP concentrations, stream sediments can act as a P sink by adsorbing SRP from the water column (McDaniel et al., 2009; Palmer-Felgate et al., 2009) whereas low SRP concentrations can favor desorption (Ezzati et al., 2020; Jarvie et al., 2005). Thus, SRP sorption/desorption in stream bed sediments is highly variable across both space and time, governed by the complex interplay between hydrology, SRP concentrations in overlying water, particle size, mineralogy and redox state (Vissers et al., 2023; Withers and Jarvie, 2008).

Seasonally fluctuating redox conditions in floodplain sediments, due to inundation and shifting groundwater table, give rise to drastically different redox activity in carbon (C) and Fe compounds that control both denitrification and SRP desorption (Peiffer et al., 2021). Floodplain inundation has been shown to increase denitrification rates (Hallberg et al., 2022; Mahl et al., 2015; McMillan and Noe, 2017) and SRP release (Loeb et al., 2008; Surridge et al., 2012; Trentman et al., 2020) but how these processes are interconnected have rarely been investigated. This is particularly important in agricultural catchments with high losses of both N and P that exacerbate eutrophication in downstream waterbodies (Conley et al., 2009). Thus, resolving the linkages and underlying drivers of N and P processing is a crucial step towards improved stream remediation and tangible water quality improvements without pollution swapping (i.e., reductions in one pollutant causing increases in another; Stevens and Quinton, 2009).

The aim of this study was to investigate the risk of SRP release from constructed floodplains across a gradient of denitrification rates and different hydrochemical conditions. The SRP exchange between sediments and water column was measured using equilibrium P concentration ($EPC_0$) incubations to compare SRP release in ten remediated reaches (floodplains) with paired unremediated reaches (stream banks). Floodplain SRP exchange was also compared with potential denitrification and $N_2O$ production rates measured previously (Hallberg et al., 2022) to investigate possible trade-offs or synergies between N and P removal. Finally, the effect of N and P processing on water quality was determined using data on water chemistry, hydrology, and catchment characteristics. We hypothesized that:

1. Floodplains increase SRP release from sediments due to higher hydrological connectivity and stronger coupling between $EPC_0$ and stream SRP concentrations, compared to stream banks of unremediated streams.
2. There is a trade-off between $NO_3^-$ and SRP removal in floodplains due to higher inundation frequency that simultaneously promotes denitrification and SRP desorption.

## 2. Materials and methods

### 2.1. Site description

Ten streams subjected to floodplain remediation (remediated streams) were selected in central east (C1–C5) and south Sweden (S6–S10; Fig. 1a; Table S1). The study sites are located in low gradient and tile drained agricultural catchments, dominated by winter and spring sown cereal crops and ley grass cultivation. Site C3 is also impacted by a chicken farm upstream of the study reach. The geology of the central east catchments (C1–C5) is characterized by crystalline bedrock, overlaid with quaternary deposits of silty clay and clay loam soil texture classes. The southern catchments (S6–S10) have limestone bedrock, overlaid with quaternary deposits of loam soil. Overall, catchments in central east (C1–C5) have lower annual precipitation, lower agricultural land use and higher clay content in soils compared to the southern catchments (S6–S10; Table S1). Remediated reaches (0.3–1.7 km) were paired with upstream unremediated control reaches, mostly of trapezoidal shape (Fig. 1b, c). Control stream reaches were selected with equivalent lengths and with similar channel slopes and agricultural land use with respect to remediated reaches. The exception was site S7 where no control stream was included since the remediated stream originates from a wetland. In addition, sites S7 and S8 are nested within the same stream network, separated by 10 km of stream length of trapezoidal shape, interspersed with remediated profiles (Fig. 1a). Floodplains in the studied remediated streams have been constructed at different elevations, ranging between 0.25 to 0.96 m above the channel bed (Table S1). Remediated streams were constructed between 2013 and 2019 by landowners and other stakeholders.

### 2.2. Sediment and water quality sampling

Sediments were sampled in autumn 2020 and spring 2021 to determine potential denitrification ($n = 109$), as part of a previous study (Hallberg et al., 2022), and during spring 2021 and 2022 to determine SRP sorption capacity ($n = 86$) and P fractions ($n = 19$); thus concurrent measurements of denitrification and $EPC_0$ were conducted only during spring 2021. We chose to measure potential rates of N and P processes in sediments with slurry methods to isolate the effect of environmental controls (inundation, water/sediment chemistry), rather than measuring in situ activity which is more dynamic and affected by site-specific confounding factors (Weigelhofer et al., 2018; Palacin-Lizarbe et al., 2020). Spring season was chosen for SRP sorption sampling to cover the period after sustained inundation during winter and spring, with maximal reducing conditions in floodplain sediments and thus highest risk of SRP desorption. Sediments for measurements of potential denitrification and $N_2O$ production activity were sampled in floodplains at up-, mid- and downstream locations in remediated reaches (Fig 1b), down to 3 cm depth with a trowel (3 $cm^3$). At each location, three pseudo-replicates were sampled within 1 $m^2$ and pooled into one sample. Briefly, potential denitrification rates were determined under anoxic conditions with substrate additions (6 mg $L^{-1}$ $NO_3^-$-N and 30 mg $L^{-1}$ C [acetate, glucose and succinate]), using an acetylene inhibition method described previously (Hallberg et al., 2022). Replicated incubations with and without acetylene were used to estimate net $N_2O$ production rates.

Sediments for measurements of SRP sorption were sampled from stream banks at upstream of control stream reaches and from floodplains at up-, mid- and downstream locations of remediated reaches, whereas sediments of stream bed and floodplains were sampled at up- and downstream for analysis of SRP sorption and P fractions (Fig. 1b, c). Stream water samples were collected in conjunction with all SRP sorption sediments for isotherm incubations. Sediments were sampled with a trowel down to 5 cm depth, covering an area of 5 × 5 cm. Depths down to 5 cm were chosen to capture the oxygenated and redox active sediment boundary at which denitrification (Roley et al., 2012) and the majority of sediment P exchange occur (Vissers et al., 2023). At floodplain and control bank locations, ten subsamples were collected with 5 m intervals along reaches. At stream bed locations, five subsamples were sampled with 10 m intervals. All sediment subsamples were pooled into one sample representing the location, placed in airtight plastic bags and

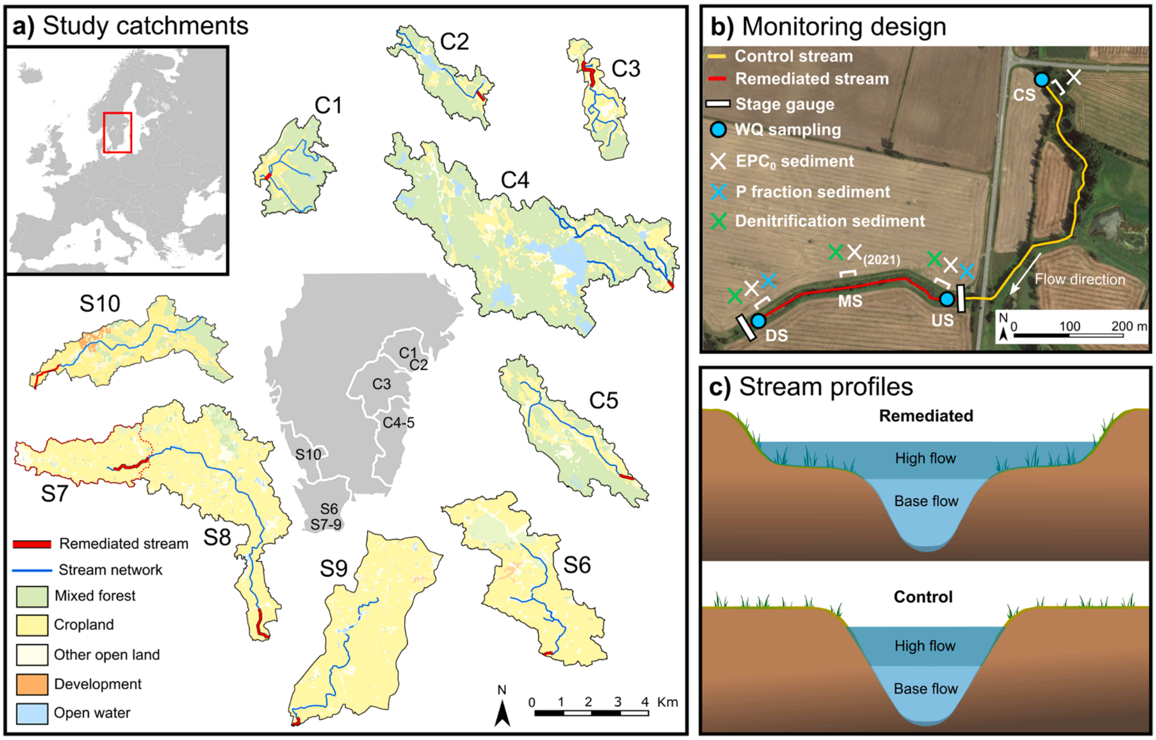


**Fig. 1.** **a)** Location of ten study catchments with remediated and control streams in central east (C1–C5) and south Sweden (S6–S10). **b)** Satellite image of reaches in site S6 showing the study design and sampling locations in control stream (CS) and remediated stream (upstream [US], midstream [MS] and downstream [DS]). **c)** Cross-sections of remediated and control streams. Satellite images: Google, ©2023 CNES / Airbus. Land use maps: ©Lantmäteriet.

stored in coolers during field transportation. Sediments were stored at 4 °C back at laboratory over 1–7 days (denitrification) and 1–2 days (P isotherm) after which dry matter (DM) was determined with oven drying over 24 h at 105 °C.

Water samples were collected monthly between April 2020 and December 2022 to determine stream water chemistry at upstream of control stream and up-, mid- and downstream of remediated streams (Fig. 1b). In site S9, samples from control reach after June 2021 were excluded from analysis due to the conversion of the control reach to a remediated reach, undertaken by landowners. Water samples were analyzed for total P (TP; SS-EN ISO 6878:2005) with and without 0.45 µm filtration, SRP ($PO_4^{3-}$-P; ISO 15,923–1:2013) with 0.45 µm filtration and $NO_3^-$-N (ISO 15,923–1:2013). Particulate P (PP) was calculated as the difference between unfiltered and filtered TP. To determine dissolved organic matter (DOM) characteristics, optical properties of water samples were measured using fluorescence and absorbance spectroscopy (Aqualog, Horiba; Hallberg et al., 2022). Dissolved oxygen (DO) and pH were measured in stream water, monthly to bimonthly, using optical and electrode-based sensors mounted to a handheld device (ProDSS, YSI).

### 2.3. P isotherms and calculation of P sorption metrics

The potential $EPC_0$ denotes at which stream water SRP concentration the net flux of SRP from sediment equals zero, i.e., neither binding nor releasing SRP (Taylor and Kunishi, 1971). Sediment $EPC_0$ was chosen as it captures the directionality and magnitude of SRP exchange, as opposed to indirect estimations from the P saturation ratio (P / Fe + aluminium [Al]). Oxalate extractions of Fe and Al are sensitive to overestimation of SRP sorption capacity by extracting not only amorphous, reactive Fe and Al oxides, but also crystalline forms with insignificant effect on P cycling (Rennert et al., 2021). Nevertheless, $EPC_0$ results should be interpreted with caution as these reflect the maximal uptake rate during complete mixing of water-sediment interface, whereas in situ conditions often exhibit different redox potentials and SRP diffusion rates in pore water (Vissers et al., 2023).

The $EPC_0$ concentration was determined with isotherm incubations of 86 sediment samples. The isotherms included four SRP solutions with target concentrations 0, 100, 250 and 500 µg $PO_4^{3-}$-P $L^{-1}$ that was prepared by mixing stream water from the different locations and a dipotassium phosphate standard ($K_2HPO_4$). SRP solutions including stream water were therefore slightly higher than target concentrations as stream water averaged 28 ± 35 µg $PO_4^{3-}$-P $L^{-1}$. We added 5 g of homogenized fresh sediments to 60 mL centrifuge tubes, together with 40 mL SRP solutions to reach a sediment to liquid ratio of 1:8. SRP solutions were stored at 4 °C for 48 h for subsequent analysis. Sediments were incubated for 24 h using an end-over-end shaker at 30 rpm and ~20 °C ambient temperature. Supernatants were then centrifuged at 2000–3000 rpm for 15–30 min, of which samples with higher clay content were centrifuged at 3000 rpm for 30 min to avoid clogging in subsequent filtering. Supernatants and stored SRP solutions were filtered (0.45 µM) and analyzed for $PO_4^{3-}$-P colorimetrically using the molybdenum blue method (Murphy and Riley, 1962). Sediment SRP sorption in mg P $kg^{-1}$ was calculated for each target concentration as initial SRP concentration subtracted with final SRP concentration after incubation, multiplied with the quotient of solution volume and sediment dry mass. Sediment $EPC_0$ was subsequently calculated by linearly or non-linearly regressing SRP sorption mass over initial SRP concentration and solving for x-intercept, equaling $EPC_0$ (Fig. S2–7). To predict SRP exchange from sediments under background SRP concentrations in stream water, P exchange potential (PEP) was calculated by subtracting $EPC_0$ with background SRP after log10-transformation (Simpson et al., 2021). Samples with $EPC_0$ value 0 ($n$ = 3) were imputed to 0.1 µg P $L^{-1}$ to calculate PEP. Sediment SRP flux under background SRP concentrations was calculated as the change in SRP mass after sediment incubation with only stream water as mg P $kg^{-1}$ DM $day^{-1}$.

### *2.4. Sequential P fractionation of sediments*

Sequential P fractionation was used to determine P forms in sediments, developed from Psenner & Puckso (1988) and Hupfer et al. (1995, 2009). The fractionation method determines operationally defined P forms of water-soluble P ($H_2O$-P), redox-sensitive P adsorbed to iron and manganese (Fe-P), $OH^-$-exchangeable P adsorbed mainly to aluminium (Al-P), P bound in organic compounds (Org-P) and calcium-bound P (Ca-P). The sum of $H_2O$-P and Fe-P fractions are referred to as labile P. Residual non-reactive P (refractory P) was not determined after fractionation, TP is here referred to as the cumulative content of all extracted P fractions. Fresh sediment samples were sequentially extracted with Milli-Q water ($H_2O$-P), buffered dithionate solution (Fe-P), NaOH (Al-P), NaOH after 30 min persulfate digestion at 120 °C, subtracted with NaOH (Org-P), and HCl (Ca-P). All extractions were analyzed for unfiltered SRP using the molybdenum blue method.

### *2.5. Hydrological monitoring and analysis*

Water stage was monitored at 10 min interval with pressure sensors (HOBO, Onset Computer Corporation) at up- and downstream locations (Fig. 1b), coupled with a sensor at field level in every site for atmospheric pressure to convert water pressure to stage. Stream discharge was measured on four to eight occasions at both locations with mid-section method using an acoustic doppler velocimeter (Flowtracker 2, SonTek) Stage-discharge rating curves were calculated according to:

$$Q = K(h + a)^p \quad (1)$$

where $Q$ is discharge ($m^3\ s^{-1}$), $h$ *is* stage (m), $a$ is stage at zero flow (m) and $K$ and $p$ are constants (Rantz, 1982). To minimize overestimation of high flows, out-of-range flows were estimated using wetted cross-section area and mean velocity (Herschy, 2014). This applied to all sites except C2 and C4 where flow was measured in conjunction to peak flows. Wetted cross-section area was modelled with polynomials of stage and cross-section area and mean velocity was modelled with logarithms of stage and mean velocity. Floodplain inundation was calculated using floodplain elevations derived from cross-section geometry surveys conducted in 2021. Annual frequency and duration of stage exceeding floodplain threshold were estimated with stage data at up- and downstream (Hallberg et al., 2022).

### *2.6. Statistical data analysis*

All statistical analyses were performed in R version 4.2.1 (RStudio Team, 2022) and significance was determined at α = 0.05. The packages hydrostats (Bond, 2022) and ContDataQC (Leppo, 2023) were used to analyze hydrological regimes. Base flow index (Gustard et al., 1992) was calculated using baseflows, and flashiness index (Baker et al., 2004) using RBIcalc.

One outlier in sediment $EPC_0$ (site C3, floodplain upstream = 249 µg $L^{-1}$) was removed from further analysis due to unrealistically high $EPC_0$ concentration. Differences in $EPC_0$, PEP and SRP flux between sediment interfaces (stream bed, floodplain and control bank) were tested using *t*-tests. SRP sorption metrics were compared separately for floodplains vs. control banks and floodplains vs. stream bed, pairing interfaces that were sampled simultaneously.

The sample distribution of predictor variables (water and floodplain sediment chemistry and catchment properties) was analyzed with scaled principal component analysis (PCA; *rda*) using the Vegan package (Oksanen et al., 2022). Vectors of $EPC_0$, PEP, SRP flux, and rates of denitrification and $N_2O$ production were fitted to the PCA using *envfit* ($R$ = 10, 000), all significantly correlated to at least one principal component axis. Based on the PCA, relationships between mean SRP concentrations in stream water, clay content and sediment Fe-P, on $EPC_0$ and denitrification were assessed. A breakpoint at > 50 inundation days $yr^{-1}$ was identified for the correlation between mean SRP concentrations and $EPC_0$.

Two outliers, one among stream water PP concentrations and one among SRP concentrations, were removed from further analysis. Site-specific comparison showed that these data points had exceptionally high concentrations (studentized residuals > 10, i.e., regression model residual divided by its adjusted standard error), which were measured in stagnant water. Water samples with SRP concentrations below detection limit of < 4 µg $L^{-1}$ (8 % of observations) were assigned to detection limit divided by 2, which has shown to be an accurate approximation for left-skewed data distributions (Hornung and Reed, 1990). The effect of location (upstream and downstream) and flow regime (base flow and inundation) on SRP and $NO_3^-$ concentrations were tested using two-way ANOVAs, performed separately for remediated and control reaches. Since the sample distributions of SRP and $NO_3^-$ concentrations did not meet the assumption of equal variances due to fewer samples during inundation, we used non-parametric permutation of two-way ANOVA ($R$ = 10,000) with *aovperm* in permuco package (Frossard and Renaud, 2021).

## 3. Results

### *3.1. Hydrological patterns and floodplain connectivity*

Annual precipitation during the study period was consistent with six-year precipitation averages at sites C3–C5, S6 and S10, whereas C1–C2 were wetter and S7–S9 were drier than normal during the study period (Table S1; SMHI, 2023). Median discharge downstream of remediated reaches were in the range < 0.01–0.21 $m^3\ s^{-1}$ and base flow index ranged between 0.20–0.45 (Table S1). Stream water inundation on floodplains occurred predominantly in winter and spring, but varied

**Table 1**
Floodplain hydrology of remediated streams (C1–C5 and S6–S10) in locations upstream (US) midstream (MS) and downstream (DS). Flow percentile of discharge (Q) at inundation onset are shown within parentheses. $Q_{50}$ = median discharge across entire study period (April 2020–December 2023).

| Site | Location | Floodplain hydrology | | | $Q_{50}$ ($m^3\ s^{-1}$) |
|---|---|---|---|---|---|
| | | Frequency (days $yr^{-1}$) | Duration (days $yr^{-1}$) | Q, inundation onset ($m^3\ s^{-1}$) | |
| C1 | US | 62 | 8 | 0.13 (86 %) | 0.05 |
| | MS | 43 | 5 | - | - |
| | DS | 249 | 47 | 0.02 (41 %) | 0.03 |
| C2 | US | 7 | 10 | 0.17 (99 %) | 0.02 |
| | MS | 16 | 7 | - | - |
| | DS | 20 | 10 | - | - |
| C3 | US | 2 | 2 | 0.53 (98 %) | < 0.01 |
| | MS | 4 | 2 | - | - |
| | DS | 49 | 6 | 0.04 (86 %) | 0.01 |
| C4 | US | 164 | 50 | 0.14 (57 %) | 0.06 |
| | MS | 179 | 43 | - | - |
| | DS | 105 | 25 | 0.49 (75 %) | 0.11 |
| C5 | US | 52 | 6 | 0.30 (91 %) | 0.02 |
| | MS | 46 | 5 | - | - |
| | DS | 32 | 4 | 0.36 (95 %) | 0.06 |
| S6 | US | 87 | 10 | 0.53 (80 %) | 0.07 |
| | MS | 111 | 20 | - | - |
| | DS | 109 | 21 | 0.41 (75 %) | 0.09 |
| S7 | US | 109 | 15 | 0.07 (75 %) | 0.01 |
| | MS | 186 | 44 | - | - |
| | DS | 149 | 25 | 0.05 (64 %) | 0.03 |
| S8 | US | 120 | 23 | 0.53 (71 %) | 0.11 |
| | MS | 186 | 51 | - | - |
| | DS | 94 | 17 | 0.62 (78 %) | 0.21 |
| S9 | US | < 1 | 1 | 1.88 (100 %) | 0.08 |
| | MS | 16 | 8 | - | - |
| | DS | 3 | 4 | 2.84 (100 %) | 0.05 |
| S10 | US | - | - | - | 0.09 |
| | MS | 80 | 6 | 0.38 (84 %) | 0.19 |
| | DS | 311 | 38 | 0.11 (23 %) | 0.19 |

greatly between sites in frequency (< 1–311 days $yr^{-1}$) and duration (1–51 days $yr^{-1}$; Table 1). Within-site variation of inundation frequency and duration was also substantial in sites C1, C3 and S10, explained by differences in floodplain elevations and channel slope. The discharge at which floodplain inundation commenced varied between sites and locations, but inundation onset consistently occurred above median discharge except downstream at S10.

### 3.2. P sorption in sediments of remediated streams

Concentrations of $EPC_0$ were consistently lower in floodplain sediments compared to control banks, indicating a lower inherent risk of SRP desorption from floodplains (Fig. 2). The same pattern applied to PEP, accounting for the influence of stream water SRP concentrations on SRP sorption. This was further corroborated by SRP fluxes under ambient stream water SRP concentrations, averaging 0.05 ± 0.26 mg P $kg^{-1}$ $day^{-1}$ in floodplain sediments and 0.38 ± 0.37 mg P $kg^{-1}$ $day^{-1}$ in control bank sediments. Nevertheless, there were no significant differences in $EPC_0$, PEP and SRP flux between floodplain and stream sediments (Fig. 2). Floodplain sediment $EPC_0$ correlated with $H_2O$-P / (Fe-P + Al-P) ($r = 0.45$, $p = 0.03$) in non-calcareous sediments (Ca-P < 0.2 g P $kg^{-1}$ DM), indicating that SRP desorption was limited by Fe and Al oxide

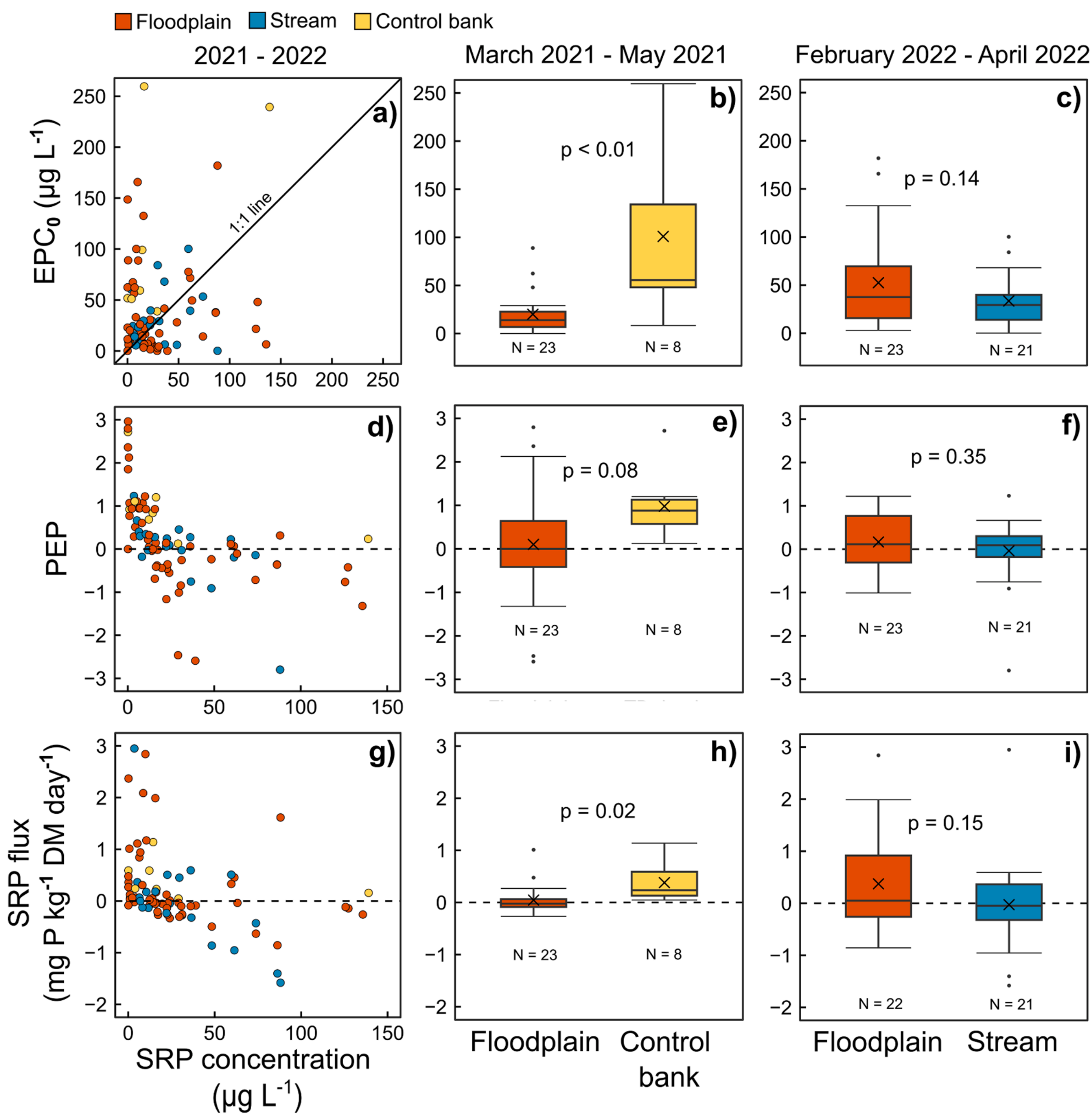


**Fig. 2.** Soluble reactive phosphorus (SRP) sorption metrics of equilibrium phosphorus concentration ($EPC_0$), phosphorus exchange potential (PEP) and SRP flux in floodplain, control bank and stream sediments. **a, d, g)** SRP sorption metrics of all sediments (2021–2022) regressed against stream water SRP concentration. **b, e, h)** Comparison of SRP sorption metrics between floodplain and control bank in spring 2021 and **c, f, i)** between stream bed and floodplain in spring 2022. Circle and box colors denote floodplain, control bank and stream sediments and p-values of *t*-tests are shown within panels with boxplots.

P saturation in absence of Ca-P co-precipitation.

Overall, SRP exchange in sediments was not in equilibrium with stream water SRP, measured at the time of sediment sampling, for any of the three interfaces (Fig. 2). Standard error in relation to 1:1 line between $EPC_0$ and SRP concentrations were lower in stream sediments ($\sigma = 34$) compared to floodplains ($\sigma = 55$) and control banks ($\sigma = 118$), suggesting limited stream water connectivity of floodplains and control banks but also limited exchange between stream water SRP and pore water SRP in stream sediments. There was no consistent temporal trend in floodplain $EPC_0$ across the sites C2–C3 and S7–S8 (Fig. S8). Instead, within-site variation at specific sampling occasions was greater than temporal variation. Further, there was no correlation between $EPC_0$ and construction year in floodplain sediments ($p = 0.39$).

### 3.3. Floodplain P sorption and denitrification controls

Denitrification potential correlated to both $EPC_0$ concentration and SRP flux in floodplain sediments when comparing means of site locations across the entire study period (Fig. 3a, b). This was also observed when comparing denitrification and SRP flux during the simultaneous sampling in spring 2021 ($r = 0.64$, $p < 0.01$, $n = 28$). By contrast, the potential $N_2O$ yield ratio of denitrification was negatively correlated to $EPC_0$ and SRP flux (Fig. 3c, d) but net $N_2O$ production rates showed no correlation with P processing. In the PCA of environmental predictors, SRP sorption capacity ($EPC_0$, PEP and SRP flux) and denitrification were associated with Fe-P content in sediments, fraction of clay in the soil, and inundation frequency (Fig. 3e). However, when regressing $EPC_0$ with individual predictors, $EPC_0$ was best explained by stream SRP mean concentration across the study period for locations with inundation frequencies of 50–300 days $yr^{-1}$ (Fig 4a). Locations with < 50 inundation days $yr^{-1}$ showed no correlation between $EPC_0$ and SRP mean concentration (Fig. 4b), suggesting that the combination of long-term SRP inputs and floodplain connectivity controlled floodplain SRP sorption. In accordance with the PCA, denitrification was correlated to Fe-P content in sediments, irrespective of inundation frequency (Fig. 4c).

### 3.4. Stream water quality responses to floodplain P processing

When testing the effect of remediated and control reaches on SRP concentrations, downstream SRP concentrations in remediated reaches were significantly reduced during base flows in sites C1, C5 and S7 (Fig. 5). By contrast, SRP concentrations were not reduced along control reaches for sites C1 and C5 (S7 no data). For $NO_3^-$ concentrations, there was no significant change along either remediated or control reaches (Fig. S9). Concentrations of SRP and $NO_3^-$ in stream water showed divergent responses to higher flows during floodplain inundation when compared to base flows. During inundation events, overall SRP concentrations both increased (site C1 and S10) and decreased (site C3 and C4; Fig. 5) while stream $NO_3^-$ concentrations consistently increased (Fig. S9).

In spring 2021, SRP desorption from floodplains of sites S8 and S10 co-occurred with increased SRP concentrations along remediated streams, compared to control streams (Table S2). However, floodplain SRP desorption in site C4 and S6–S7 resulted in either no change or net retention of SRP concentrations. In spring 2022, trends in SRP sorption at site C2–C3 and S7–S8 were consistent with spring 2021, but stream water SRP concentration in site C2 switched from increases in 2021 to reductions in 2022.

## 4. Discussion

### 4.1. Sediment P exchange across the stream corridor

Floodplains in agricultural streams reduced the potential for SRP release compared to stream banks in unremediated streams, contrary to

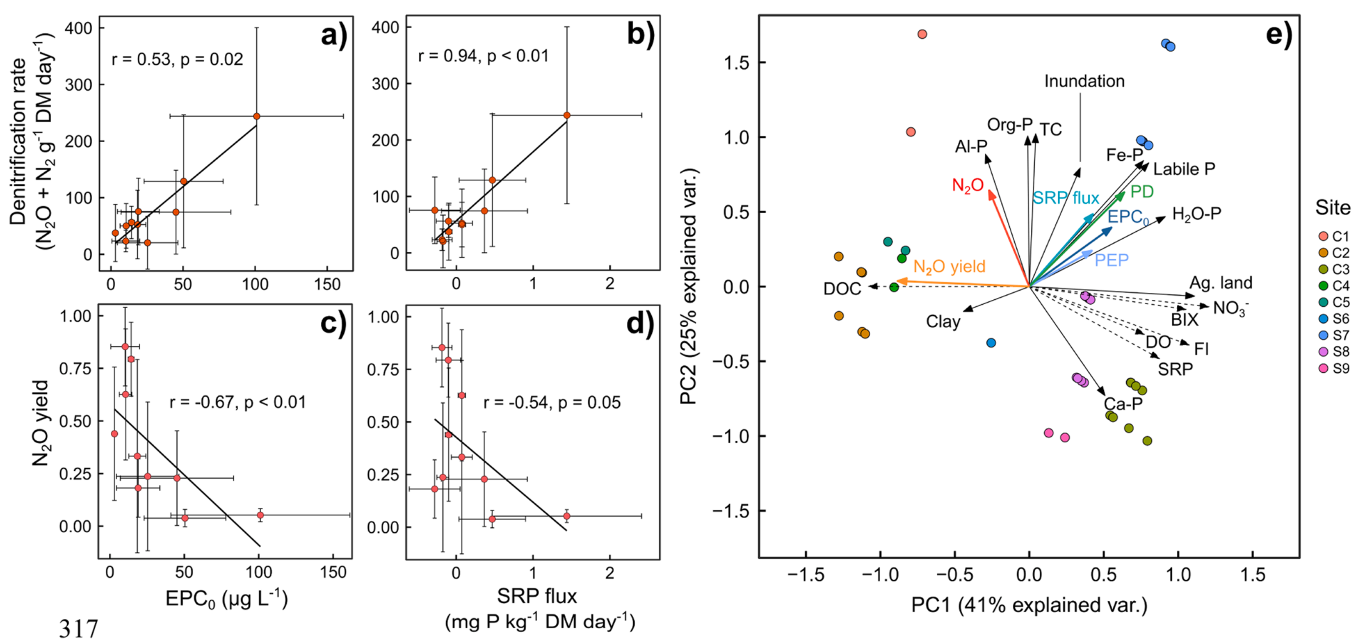


**Fig. 3.** Relationship between soluble reactive phosphorus (SRP) sorption and denitrification in floodplain sediments. Linear regression of means for each site location between **a)** potential denitrification (PD) and equilibrium phosphorus concentration ($EPC_0$) and **b)** PD and SRP flux, **c)** nitrous oxide ($N_2O$) yields and $EPC_0$ and **d)** $N_2O$ yields and SRP flux. Standard deviation is shown as whiskers. **e)** Principal component analysis of environmental predictor variables. The processes $EPC_0$, phosphorus exchange potential (PEP), SRP flux, PD rate, potential $N_2O$ rate and $N_2O$ yield ratio were significantly ($p < 0.05$) correlated with the environmental structure and shown as vectors, with lengths proportional to the strength of the correlation. Solid black vectors denote catchment and sediment properties, and dashed black vectors denote water properties. Colored vectors denote response variables and circle color denotes sampling site. Samples with missing variables were removed from the analysis and all descriptor variables were standardized to equal standard deviations. Water variables are means of samples from April 2020 to December 2022. Denitrification was sampled in September 2020 to May 2021 and $EPC_0$ and SRP flux in March 2021 to April 2022. DO = dissolved oxygen, $NO_3^-$-*N* = nitrate-nitrogen, DOC = dissolved organic carbon, FI = fluorescence index, BIX = biological freshness index, TC = Total carbon in sediments.

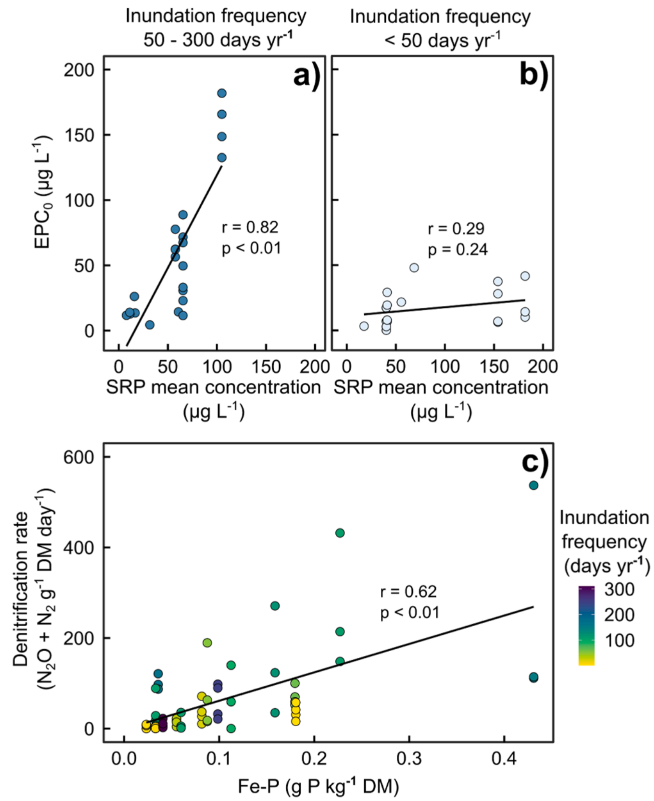


**Fig. 4.** Relationship between equilibrium phosphorus concentration ($EPC_0$) and soluble reactive phosphorus (SRP) mean concentrations of the study period, in locations with inundation frequencies **a)** 50–300 and **b)** < 50 days $yr^{-1}$. **c)** Relationship between denitrification and phosphorus associated to iron oxides (Fe-P), showing floodplain inundation frequency as a continuous gradient.

our hypothesis. Floodplain remediation introduces a qualitatively different riparian interface that enables longer solute residence time, which likely supports a higher capacity for biogeochemical processing of SRP compared to trapezoidal, steep banks of unremediated streams. The SRP exchange from floodplain sediments, shaped by periodic inundation events, was comparable to that of stream sediments and overall close to net zero SRP release under ambient stream water SRP concentrations. Although stream bank sediments can be SRP sources (Ezzati et al., 2020; Kindervater and Steinman, 2019), $EPC_0$ of unremediated stream banks and stream SRP concentrations were decoupled in this study. This demonstrates that hydrological connectivity across the stream corridor regulates the extent to which SRP can be exchanged. Desorption of SRP from stream banks is thus restricted by its limited interaction with the water column and it is more likely that stream banks had a greater impact on water quality through erosion and mobilization of PP (Hallberg et al., 2024; Fox et al., 2016). However, when stream water comes in contact with stream banks, their high $EPC_0$ implies a higher risk for SRP release, compared to floodplains. In accordance with our results, hydrological connectivity has previously been identified as the main determinant for SRP desorption in nutrient-impacted catchments, including small headwater floodplains (McMillan and Noe, 2017; Trentman et al., 2020) and large riverine floodplains (Preiner et al., 2020). The recently exposed sediments of floodplains, previously constituting subsoil, did not differ from stream sediments in P content, and we did not observe any evidence of accumulation of leached Fe and Al oxides in floodplain sediments (Daly et al., 2017). This could explain why floodplain SRP sorption did not surpass that of the stream bed, contrasting previous observations (Trentman et al., 2020). Besides geochemical processes, biotic SRP turnover can also substantially affect SRP concentrations in impacted streams (Stutter et al., 2010; Simpson et al., 2020). In particular, SRP assimilation by floodplain vegetation has been proposed as a P sink during growing season, with the potential to buffer elevated risks of SRP desorption during spring months (Trentman et al., 2020). The combined analysis of assimilatory uptake and geochemical sorption could therefore provide additional insights into the complementarity of biotic and abiotic SRP processing in floodplains.

### 4.2. Trade-off between N and P removal in floodplain sediments

The correlation between potential rates of denitrification and SRP desorption in floodplain sediments confirmed our hypothesis that higher $NO_3^-$ removal coincides with SRP release under inundated conditions. This trade-off in N and P removal was observed both when comparing denitrification and SRP desorption over the study period as well as the simultaneous sampling period in spring 2021. This finding links these two processes with higher hydrological connectivity to floodplains and implies that SRP release does not increase under lower $NO_3^-$ concentrations and denitrification rates, as reported in N-limited forested catchments (Musolff et al., 2017). Although the potential process rates of N and P measured in this study do not necessarily reflect in situ floodplain fluxes, they capture the time-integrated response to underlying environmental controls. As such, potential rates are more suitable for identifying drivers of nutrient processing across sites, compared to the more dynamic in situ migration rates affected by local, site-specific confounding factors (Weigelhofer et al., 2018; Palacin-Lizarbe et al., 2020).

Net $N_2O$ production rates in floodplain sediments, accounting for 35 % of the rates across the stream system (Hallberg et al., 2022), was not influenced by shifts in the balance between denitrification and SRP desorption. Although relative $N_2O$ yields decreased with higher SRP desorption, $N_2O$ yields primarily indicated that the efficiency of complete reduction of $NO_3^-$ increased with higher denitrification rates.

The correlation between potential denitrification and Fe-P content in sediments may be indicative of reducing conditions that enable both $NO_3^-$ and Fe oxide reduction. However, $Fe^{2+}$ can be used as an electron donor in denitrification, thereby increasing $NO_3^-$ removal in floodplains with higher Fe oxide concentrations (Nielsen and Nielsen, 1998). Besides the link to Fe-P, denitrification rates were mainly predicted by the proportion of agricultural land in the catchment, as discussed in Hallberg et al. (2022).

### 4.3. Hydrochemical and soil drivers of P processing in floodplains

Floodplain sediment $EPC_0$ was controlled by long-term mean stream water SRP concentration in locations where floodplains were subjected to recurring inundation (50–300 days $yr^{-1}$). Although there was a pattern of increased $EPC_0$ with Fe-P content in sediments, this was not consistent across locations with recurring inundation. High Fe-P content suggests large labile P stores but this can coincide with additional free binding sites of Al oxides and clay minerals that maintain a low $EPC_0$. Accordingly, soils with > 40 % clay showed the lowest $EPC_0$ concentrations, likely explained by the higher proportion of Al-P and lower proportion of Fe-P, compared to loamy and sandy soils. Thus, the resilience to SRP desorption in inundated clay soils is facilitated by greater SRP sorption to Al oxides and clay minerals, with divergent pH dependency compared to Fe oxides (Gérard, 2016). This further implies that coarser soils, poor in Al, are more dependent on SRP sorption to Fe oxides and therefore more vulnerable to fluctuating redox conditions and SRP release, as previously shown by Djodjic et al. (2021, 2023). The switch from sink to source of SRP in loamy and sandy soils occurred at 75 days inundation days $yr^{-1}$, corresponding to a mean duration of 12 days. This was longer than previous estimates of 6 (Surridge et al., 2012) to 7 days (Scalenghe et al., 2002) of water-logged conditions, required to initiate SRP desorption. Transient redox regimes in aquatic systems have been hypothesized to increase the release of redox-active elements with temporarily thermodynamically unstable states, with mixed phases

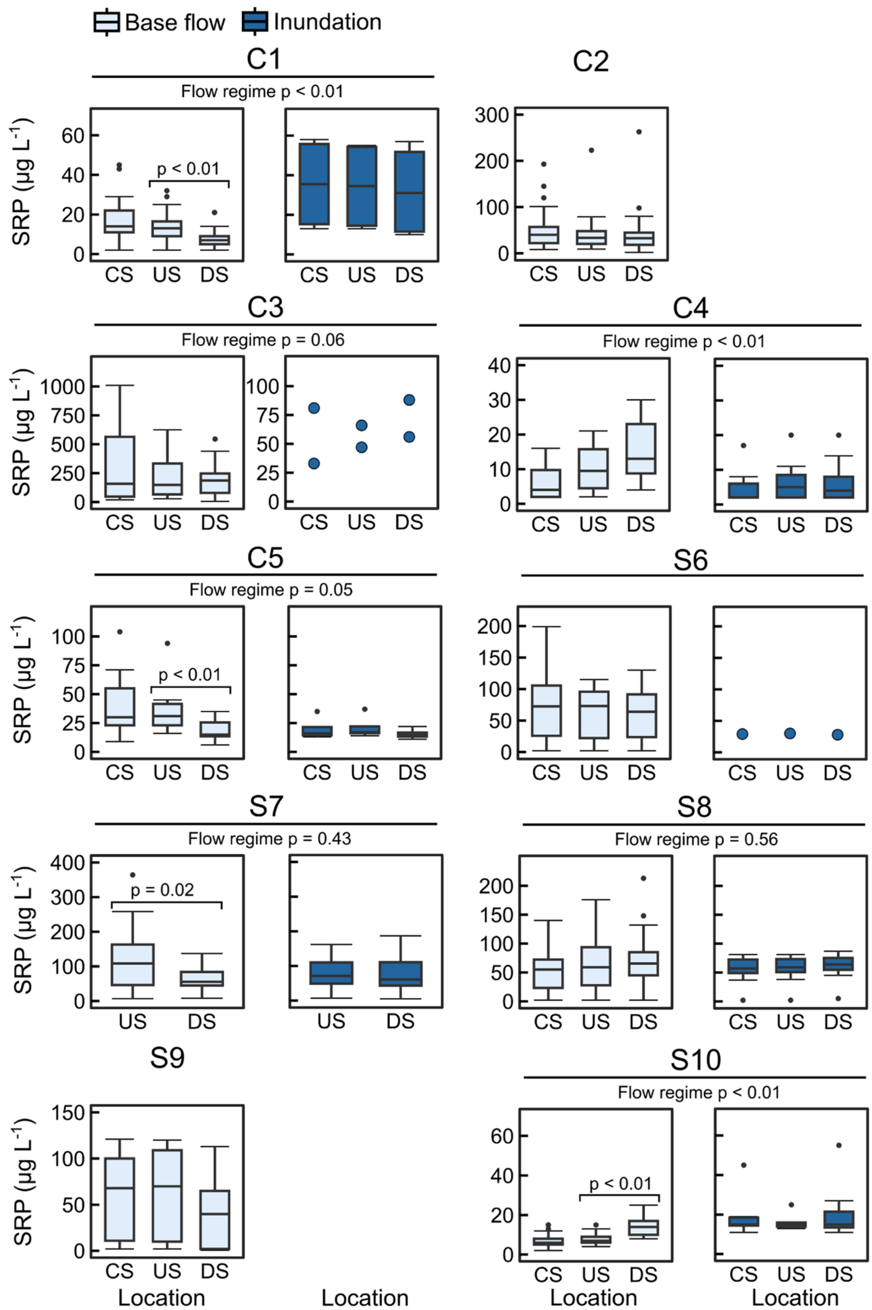


**Fig. 5.** Stream water concentrations of soluble reactive phosphorus (SRP) in the control stream (CS) and upstream (US) and downstream (DS) of remediated reaches, during base flows and inundation events. P-values of one-way ANOVAs with site-specific flow regime as factor are shown above the panels, whereas p-values of *t*-tests ($p < 0.05$) of SRP concentrations between CS and US (control reach) and US and DS (remediated reach) are shown within panels.

capable of both donating and accepting electrons that can greatly enhance rates of both SRP sorption and denitrification (Peiffer et al., 2021). Our results are consistent with this concept, showing that inundation is a critical control for floodplain nutrient processing, particularly in coarser soils compared to clay soils.

### *4.4. Linking floodplain P processing to water quality*

The impact of floodplain SRP desorption on stream water SRP concentrations during spring season was limited, with only two sites (S8 and S10) showing a concurrent increase in floodplain SRP desorption and stream SRP concentrations. The ratio of SRP:TP concentrations was on average 31 ± 23 % for all sites, demonstrating that PP was the predominant P form (except in site C3: 67 %) and thus more influential on TP transport in these streams. Accordingly, the SRP release in site S8 was offset by PP reductions, suggesting that geomorphological fluvial processes exert a stronger influence on P exports (Hallberg et al., 2024). This is consistent with a previous study that identified PP mobilization as more important for P turnover during storm events, compared to SRP desorption (Li et al., 2023). In the other sites dominated by SRP desorption (C4 and S6–S7), SRP concentrations were reduced or unchanged despite frequent inundation (> 90 days $yr^{-1}$). Here, vertical transport of released SRP following inundation by advective draw-down could have counteracted the impact of SRP release to the water column (Surridge et al., 2012). In addition, Al-P and Org-P content were significantly higher in site S7, which indicates that SRP at this site could be bound to these fractions following desorption from Fe-P. We also note that the estimation of $EPC_0$ using constant mixing of water and sediments reflects SRP exchange during resuspension of sediments, which likely overestimates the in situ interaction between water column and sediments (Stutter et al., 2010; Weigelhofer et al., 2018).

At monthly to seasonal scales, inundation periods did not produce any changes in SRP concentrations between remediated and unremediated reaches. Because inundation is dependent on hydrology, higher flows during inundation events can decrease solute residence times and to some extent short-circuit SRP exchange with sediments (House, 2003). Overall, there was no consistent response in SRP concentrations to inundation; only two sites (C1 and S10) showed increasing SRP concentrations with higher flows. This suggests differences in transport and source limitations across sites, with different contributions from diffuse and point sources. The dilution of SRP concentrations with higher flows (C3-C5 and S6) indicates a lower relative contribution from point sources (Bowes et al., 2008). Although no systematic investigation of point sources has been carried out in the study catchments, site C3 was most likely affected by point release of SRP from a chicken farm in the catchment, leading to high SRP concentrations during base flows and their dilution at higher flows.

Floodplain sediment $EPC_0$ was measured in spring because this period was expected to show the highest reducing conditions and elevated risk for SRP desorption due to prolonged floodplain inundation (Loeb et al., 2008). Correspondingly, denitrification rates in floodplain sediments of the sites in the current study peaked in spring (Hallberg et al., 2022). Although previous studies show inconsistent patterns in floodplain $EPC_0$ from spring to autumn (Kindervater and Steinman, 2019; Trentman et al., 2020), seasonal variations in stream water SRP concentration are likely exerting the highest influence on sediment SRP exchange (Jarvie et al., 2005). Peaks in SRP concentration occurred in summer/autumn and minima in spring which further confirmed the latter period as the most sensitive for sediment SRP release. Floodplain SRP exchange can further be dynamic at finer temporal resolution, such as during single inundation events. A previous study showed that during the onset of inundation, SRP sorption dominated, while prolonged inundation duration resulted in SRP desorption (Preiner et al., 2020). To capture this initial buffering effect across daily to weekly intervals, high-frequency sampling techniques can be required to reveal hot moments of sorption/desorption that impact water quality disproportionally (Bieroza et al., 2023).

## 5. Conclusions

Floodplain remediation extends the often-restricted riparian zones of agricultural streams and leverages hydrological and biogeochemical processes to enhance nutrient and sediment removal. By linking N and P processing in floodplains, this study contributes a novel perspective on antagonistic responses of $NO_3^-$ and SRP and removal upon inundation, resulting in pollution swapping between the two macro nutrients that mainly limit primary production in freshwaters. Reduced conditions in floodplain sediments, promoted by periodical stream water overflow, enhanced microbial removal of $NO_3^-$ at the expense of increased geochemical SRP desorption. However, these processes only responded to floodplain inundation in sediments on loamy and sandy soils, indicating that sediments with underlying clay soils were either source-limited or buffered SRP release while also restraining denitrification. Overall, SRP exchange from floodplains during spring season did not differ from stream sediments. However, in sites where SRP desorption from floodplains dominated, the combination of prolonged inundation, high SRP inputs over time and coarser soils led to increased stream water SRP concentrations along remediated reaches. When implementing floodplain remediation in agricultural streams, it is therefore important that both soil texture and dominating nutrient forms ($NO_3^-$, SRP and PP) guide the choice of appropriate placement and floodplain design to improve stream water quality.

## CRediT authorship contribution statement

**Lukas Hallberg:** Conceptualization, Data curation, Formal analysis, Methodology, Visualization, Writing – original draft, Writing – review & editing. **Sara Hallin:** Formal analysis, Methodology, Writing – review & editing. **Faruk Djodjic:** Formal analysis, Methodology, Writing – review & editing. **Magdalena Bieroza:** Conceptualization, Formal analysis, Funding acquisition, Methodology, Writing – review & editing.

## Declaration of competing interest

The authors declare that they have no known competing financial interests or personal relationships that could have appeared to influence the work reported in this paper.

## Data availability

Data will be made available on request.

## Acknowledgements

This work was funded by Svenska Forskningsrådet Formas (2018–00890), Havs- och vattenmyndigheten (3280–2019), and Oscar och Lili Lamms Minne (DO2019–0021) awarded to M. Bieroza. The authors would like to thank private landowners and stakeholders in the study catchments for their help with collecting water and sediments samples and providing access to field sites, especially Christoffer Bonthron from Tullstorpsåprojektet, Anuschka Heeb from Lovang AB and Dennis Wiström from Västerviks kommun. We thank Sheryl Illao Åström for conducting the geometrical surveys and compiling GPS data. We also thank Emilien Casali, Linus Holgersson, and Emma Ryding for collecting sediments, performing isotherm incubations, and sequential P fractionation.

## Supplementary materials

Supplementary material associated with this article can be found, in the online version, at doi:10.1016/j.watres.2024.121770.

## References

Baker, D.B., Richards, R.P., Loftus, T.T., Kramer, J.W., 2004. A new flashiness index: characteristics and applications to midwestern rivers and streams1. JAWRA 40 (2), 503–522.
Basu, N.B., Van Meter, K.J., Byrnes, D.K., Van Cappellen, P., Brouwer, R., Jacobsen, B.H., Jarsjö, J., Rudolph, D.L., Cunha, M.C., Nelson, N., Bhattacharya, R., Destouni, G., Olsen, S.B., 2022. Managing nitrogen legacies to accelerate water quality improvement. Nat. Geosci 15 (2), 97–105.
Bieroza, M., Acharya, S., Benisch, J., ter Borg, R.N., Hallberg, L., Negri, C., Pruitt, A., Pucher, M., Saavedra, F., Staniszewska, K., van't Veen, S.G.M., Vincent, A., Winter, C., Basu, N.B., Jarvie, H.P., Kirchner, J.W., 2023. Advances in catchment science, hydrochemistry, and aquatic ecology enabled by high-frequency water quality measurements. Environ. Sci. Technol. 57 (12), 4701–4719.
Bieroza, M.Z., Bol, R., Glendell, M., 2021. What is the deal with the Green Deal: will the new strategy help to improve European freshwater quality beyond the water framework directive? Sci. Total Environ. 791, 148080.
Bond, N. (2022). Hydrostats: hydrologic indices for daily time series data. https://CRAN.R-project.org/package=hydrostats [accessed 26 January 2024].
Bowes, M.J., Smith, J.T., Jarvie, H.P., Neal, C., 2008. Modelling of phosphorus inputs to rivers from diffuse and point sources. Sci. Total Environ 395 (2–3), 125–138.
Bukaveckas, P.A., 2007. Effects of channel restoration on water velocity, transient storage, and nutrient uptake in a channelized stream. Environ. Sci. Technol. 41 (5), 1570–1576.
Conley, D.J., Paerl, H.W., Howarth, R.W., Boesch, D.F., Seitzinger, S.P., Havens, K.E., Lancelot, C., Likens, G.E., 2009. Controlling eutrophication: nitrogen and phosphorus. Science 323 (5917), 1014–1015.
Daly, K., Tuohy, P., Peyton, D., Wall, D.P., Fenton, O., 2017. Field soil and ditch sediment phosphorus dynamics from two artificially drained fields on poorly drained soils. Agricul. Water Manag 192, 115–125.
Djodjic, F., Bergström, L., Schmieder, F., Sandström, C., Agback, P., Hu, Y., 2023. Soils potentially vulnerable to phosphorus losses: speciation of inorganic and organic

phosphorus and estimation of leaching losses. Nutr. Cycl. Agroecosy 127 (2), 225–245.
Djodjic, F., Bieroza, M., Bergström, L., 2021. Land use, geology and soil properties control nutrient concentrations in headwater streams. Sci. Total Environt 772, 145108.
Ezzati, G., Fenton, O., Healy, M.G., Christianson, L., Feyereisen, G.W., Thornton, S., Chen, Q., Fan, B., Ding, J., Daly, K., 2020. Impact of P inputs on source-sink P dynamics of sediment along an agricultural ditch network. J. Environ. Manage. 257, 109988.
Fox, G.A., Purvis, R.A., Penn, C.J., 2016. Streambanks: a net source of sediment and phosphorus to streams and rivers. J. Environ. Manage. 181, 602–614.
Frossard, J., Renaud, O., 2021. Permutation tests for regression, ANOVA, and comparison of signals: the permuco package. J. Stat. Softw 99, 1–32.
Gérard, F., 2016. Clay minerals, iron/aluminum oxides, and their contribution to phosphate sorption in soils—a myth revisited. Geoderma 262, 213–226.
Glibert, P.M., Maranger, R., Sobota, D.J., Bouwman, L., 2014. The haber bosch–harmful algal bloom (HB–HAB) link. Environmen. Res. Lett 9 (10), 105001.
Gustard, A., Bullock, A., Dixon, J.M., 1992. Low flow estimation in the United Kingdom. Inst. Hydrol.
Hallberg, L., Djodjic, F., Bieroza, M., 2024. Phosphorus supply and floodplain design govern phosphorus reduction capacity in remediated agricultural streams. Hydrol. Earth Syst. Sci 28 (2), 341–355.
Hallberg, L., Hallin, S., Bieroza, M., 2022. Catchment controls of denitrification and nitrous oxide production rates in headwater remediated agricultural streams. Sci. Total Environ 838, 156513.
Herschy, R.W., 2014. Streamflow Measurement, 3rd ed. CRC Press.
Hornung, R.W., Reed, L.D., 1990. Estimation of average concentration in the presence of nondetectable values. Appl. Occup. Environ. Hyg 5 (1), 46–51.
House, W.A., 2003. Geochemical cycling of phosphorus in rivers. Appl. Geochem. 18 (5), 739–748.
Hupfer, M., Gächter, R., Giovanoli, R., 1995. Transformation of phosphorus species in settling seston and during early sediment diagenesis. Aquat. Sci 57 (4), 305–324.
Hupfer, M., Zak, D., Roβberg, R., Herzog, C., Pöthig, R., 2009. Evaluation of a well-established sequential phosphorus fractionation technique for use in calcite-rich lake sediments: identification and prevention of artifacts due to apatite formation. Methods 7 (6), 399–410.
Jarvie, H.P., Jürgens, M.D., Williams, R.J., Neal, C., Davies, J.J.L., Barrett, C., White, J., 2005. Role of river bed sediments as sources and sinks of phosphorus across two major eutrophic UK river basins: the Hampshire Avon and Herefordshire Wye. J. Hydrol. (Amst) 304 (1), 51–74.
Keiser, D.A., Shapiro, J.S., 2019. Consequences of the clean water act and the demand for water quality. Q. J. Econ 134 (1), 349–396.
Kindervater, E., Steinman, A.D., 2019. Two-stage agricultural ditch sediments act as phosphorus sinks in West Michigan. JAWRA 55 (5), 1183–1195.
Le Moal, M., Gascuel-Odoux, C., Ménesguen, A., Souchon, Y., Étrillard, C., Levain, A., Moatar, F., Pannard, A., Souchu, P., Lefebvre, A., Pinay, G, 2019. Eutrophication: a new wine in an old bottle? Sci. Total Environ 651, 1–11.
Leppo, E. (2023). ContDataQC: quality control (QC) of continous monitoring data. https://github.com/leppott/ContDataQC/.
Li, S., Arnscheidt, J., Cassidy, R., Douglas, R.W., McGrogan, H.J., Jordan, P., 2023. The spatial and temporal dynamics of sediment phosphorus attenuation and release in impacted stream catchments. Water Res. 245, 120663.
Loeb, R., Lamers, L.P.M., Roelofs, J.G.M., 2008. Prediction of phosphorus mobilisation in inundated floodplain soils. Environmen. Poll 156 (2), 325–331.
Mahl, U.H., Tank, J.L., Roley, S.S., Davis, R.T., 2015. Two-stage ditch floodplains enhance n-removal capacity and reduce turbidity and dissolved P in agricultural streams. JAWRA 51 (4), 923–940.
McDaniel, M.D., David, M.B., Royer, T.V., 2009. Relationships between benthic sediments and water column phosphorus in illinois streams. J. Environ. Qual. 38 (2), 607–617.
McMillan, S.K., Noe, G.B., 2017. Increasing floodplain connectivity through urban stream restoration increases nutrient and sediment retention. Ecol. Eng 108, 284–295.
Murphy, J., Riley, J.P., 1962. A modified single solution method for the determination of phosphate in natural waters. Anal. Chim. Acta 27, 31–36.
Musolff, A., Selle, B., Büttner, O., Opitz, M., Tittel, J., 2017. Unexpected release of phosphate and organic carbon to streams linked to declining nitrogen depositions. Glob. Chang. Biol 23 (5), 1891–1901.
Nielsen, J.L., Nielsen, P.H., 1998. Microbial nitrate-dependent oxidation of ferrous iron in activated sludge. Environ. Sci. Technol. 32 (22), 3556–3561.
Oksanen, J., Simpson, G., Blanchet, F., Kindt, R., Legendre, P., Minchin, P., O'Hara, R., Solymos, P., Stevens, M., Szoecs, E., Wagner, H., Barbour, M., Bedward, M., Bolker, B., Borcard, D., Carvalho, G., Chirico, M., De Caceres, M., Durand, S., Evangelista, H., FitzJohn, R., Friendly, M., Furneaux, B., Hannigan, G., Hill, M., Lahti, L., McGlinn, D., Ouellette, M., Ribeiro Cunha, E., Smith, T., Stier, A., Ter Braak, C., & Weedon, J. (2022). Vegan: community ecology package. https://CRAN.R-project.org/package=vegan [accessed: 26 January 2024].
Palacin-Lizarbe, C., Camarero, L., Hallin, S., Jones, C.M., Catalan, J., 2020. Denitrification rates in lake sediments of mountains affected by high atmospheric nitrogen deposition. Sci. Rep 10 (1), 3003.
Palmer-Felgate, E.J., Jarvie, H.P., Withers, P.J.A., Mortimer, R.J.G., Krom, M.D., 2009. Stream-bed phosphorus in paired catchments with different agricultural land use intensity. Agric. Ecosyst. Environ 134 (1), 53–66.
Peiffer, S., Kappler, A., Haderlein, S.B., Schmidt, C., Byrne, J.M., Kleindienst, S., Vogt, C., Richnow, H.H., Obst, M., Angenent, L.T., Bryce, C., McCammon, C., Planer-Friedrich, B., 2021. A biogeochemical–hydrological framework for the role of redox-active compounds in aquatic systems. Nat. Geosci 14 (5), 264–272.
Powell, G.E., Ward, A.D., Mecklenburg, D.E., Jayakaran, A.D., 2007. Two-stage channel systems: part 1, a practical approach for sizing agricultural ditches. J. Soil Water Conser 10, 277–286.
Preiner, S., Bondar-Kunze, E., Pitzl, B., Weigelhofer, G., Hein, T., 2020. Effect of hydrological connectivity on the phosphorus buffering capacity of an urban floodplain. Front. Environmen. Sci 721, 137620.
Psenner, R., Pucksko, R., 1988. Phosphorus fractionation: advantages and limits of the method for the study of sediment P origins and interactions. Arch. Hydrobiol 30, 43–59.
Rantz, S.E., 1982. Measurement and computation of streamflow. In: Measurement and Computation of Streamflow (USGS Numbered Series 2175, 2175. Water Supply Paper.
Rennert, T., Dietel, J., Heilek, S., Dohrmann, R., Mansfeldt, T., 2021. Assessing poorly crystalline and mineral-organic species by extracting Al, Fe, Mn, and Si using (citrate-) ascorbate and oxalate. Geoderma 397, 115095.
Riseng, C.M., Wiley, M.J., Black, R.W., Munn, M.D., 2011. Impacts of agricultural land use on biological integrity: a causal analysis. Ecolog. Applic 21 (8), 3128–3146.
Roley, S.S., Tank, J.L., Stephen, M.L., Johnson, L.T., Beaulieu, J.J., Witter, J.D., 2012. Floodplain restoration enhances denitrification and reach-scale nitrogen removal in an agricultural stream. Ecolog. Applic 22 (1), 281–297.
Roley, S.S., Tank, J.L., Tyndall, J.C., Witter, J.D., 2016. How cost-effective are cover crops, wetlands, and two-stage ditches for nitrogen removal in the Mississippi River Basin? Water Resour. Econ 15, 43–56.
Team, RStudio, 2022. RStudio: Integrated Development For R. RStudio, Inc, Boston, MA. URL. http://www.rstudio.com/ [accessed 26 January 2024].
Scalenghe, R., Edwards, A.C., Ajmone Marsan, F., Barberis, E., 2002. The effect of reducing conditions on the solubility of phosphorus in a diverse range of European agricultural soils. Eur. J. Soil Sci 53 (3), 439–447.
Sharpley, A., Jarvie, H.P., Buda, A., May, L., Spears, B., Kleinman, P., 2013. Phosphorus legacy: overcoming the effects of past management practices to mitigate future water quality impairment. J. Environ. Qual. 42 (5), 1308–1326.
Simpson, Z.P., McDowell, R.W., Condron, L.M., 2020. The biotic contribution to the benthic stream sediment phosphorus buffer. Biogeochemistry 151 (1), 63–79.
Simpson, Z.P., McDowell, R.W., Condron, L.M., McDaniel, M.D., Jarvie, H.P., Abell, J.M., 2021. Sediment phosphorus buffering in streams at baseflow: a meta-analysis. J. Environ. Qual. 50 (2), 287–311.
SMHI, 2023. Ladda ner meteorologiska observationer. Swed. Meteorolog. Hydrolog. Inst. https://www.smhi.se/data/meteorologi/ladda-ner-meteorologiska-observationer#param=airtemperatureInstant,stations=core [accessed 26 January 2024].
Stevens, C.J., Quinton, J.N., 2009. Diffuse pollution swapping in arable agricultural systems. Crit. Rev. Environ. Sci. Technol 39 (6), 478–520.
Stutter, M.I., Demars, B.O.L., Langan, S.J., 2010. River phosphorus cycling: separating biotic and abiotic uptake during short-term changes in sewage effluent loading. Water Res. 44 (15), 4425–4436.
Surridge, B.W.J., Heathwaite, A.L., Baird, A.J., 2012. Phosphorus mobilisation and transport within a long-restored floodplain wetland. Ecol. Eng 44, 348–359.
Taylor, A.W., Kunishi, H.M., 1971. Phosphate equilibria on stream sediment and soil in a watershed draining an agricultural region. J. Agric. Food Chem. 19 (5), 827–831.
Trentman, M.T., Tank, J.L., Jones, S.E., McMillan, S.K., Royer, T.V., 2020. Seasonal evaluation of biotic and abiotic factors suggests phosphorus retention in constructed floodplains in three agricultural streams. Sci. Total Environ 729, 138744.
Vissers, M.A., Roy, J.W., Yates, A.G., Robinson, K., Rakhimbekova, S., Robinson, C.E., 2023. Simps. J. Hydrol. (Amst) 617, 129133.
Weigelhofer, G., Ramião, J.P., Pitzl, B., Bondar-Kunze, E., O'Keeffe, J, 2018. Decoupled water-sediment interactions restrict the phosphorus buffer mechanism in agricultural streams. Sci. Total Environ 628, 44–52.
Withers, P.J.A., Jarvie, H.P., 2008. Delivery and cycling of phosphorus in rivers: a review. Sci. Total Environ 400 (1), 379–395.